

# Eighteen mega-electron-volt alpha-particle damage in homoepitaxial $\beta$ -Ga<sub>2</sub>O<sub>3</sub> Schottky rectifiers

Jiancheng Yang, Chaker Fares, Yu Guan, F. Ren, S. J. Pearton, Jinho Bae, Jihyun Kim, and Akito Kuramata

Citation: *Journal of Vacuum Science & Technology B* **36**, 031205 (2018); doi: 10.1116/1.5027613

View online: <https://doi.org/10.1116/1.5027613>

View Table of Contents: <http://avs.scitation.org/toc/jvb/36/3>

Published by the *American Vacuum Society*

---

---



Contact Hiden Analytical for further details:  
W [www.HidenAnalytical.com](http://www.HidenAnalytical.com)  
E [info@hiden.co.uk](mailto:info@hiden.co.uk)

**CLICK TO VIEW** our product catalogue

## Instruments for Advanced Science



**Gas Analysis**

- dynamic measurement of reaction gas streams
- catalysis and thermal analysis
- molecular beam studies
- dissolved species probes
- fermentation, environmental and ecological studies




**Surface Science**

- UHV TPD
- SIMS
- end point detection in ion beam etch
- elemental imaging - surface mapping



**Plasma Diagnostics**

- plasma source characterization
- etch and deposition process reaction kinetic studies
- analysis of neutral and radical species



**Vacuum Analysis**

- partial pressure measurement and control of process gases
- reactive sputter process control
- vacuum diagnostics
- vacuum coating process monitoring

# Eighteen mega-electron-volt alpha-particle damage in homoepitaxial $\beta$ -Ga<sub>2</sub>O<sub>3</sub> Schottky rectifiers

Jiancheng Yang, Chaker Fares, Yu Guan, and F. Ren

*Department of Chemical Engineering, University of Florida, Gainesville, Florida 32611*

S. J. Pearton<sup>a)</sup>

*Department of Materials Science and Engineering, University of Florida, Gainesville, Florida 32611*

Jinho Bae and Jihyun Kim

*Department of Chemical and Biological Engineering, Korea University, Seoul 136-713, South Korea*

Akito Kuramata

*Tamura Corporation and Novel Crystal Technology, Inc., Sayama, Saitama 350-1328, Japan*

(Received 4 March 2018; accepted 23 April 2018; published 8 May 2018)

Homoepitaxial Ga<sub>2</sub>O<sub>3</sub> rectifiers with vertical geometry were subject to 18 MeV alpha particle irradiation at fluences of  $10^{12}$ – $10^{13}$  cm<sup>-2</sup>, simulating space radiation exposure. The range of these particles ( $\sim 80$   $\mu$ m) is much greater than the drift layer thickness in the structures ( $\sim 7$   $\mu$ m). The carrier removal rates were in the range of 406–728 cm<sup>-1</sup> for these conditions. These values are factors of 2–3 higher than for high energy (10 MeV) protons and 2 orders of magnitude higher than for 1.5 MeV electron irradiation of the same material. The on-state resistance of the rectifiers is more degraded by alpha particle irradiation than either ideality factor or barrier height. The reverse breakdown voltage of the rectifiers increases with alpha particle dose as carriers in the drift region are removed by trapping into traps created by the radiation damage. The on/off ratio of the rectifiers was severely degraded by alpha particle-induced damage, but the reverse recovery characteristics were unaffected even by the highest dose, with values around  $\sim 20$  ns. *Published by the AVS.*  
<https://doi.org/10.1116/1.5027613>

## I. INTRODUCTION

There is currently significant interest in the use of  $\beta$ -Ga<sub>2</sub>O<sub>3</sub> for ultrahigh power electronics and solar blind photodetectors.<sup>1–17</sup> The  $\beta$ -polymorph can be readily grown in the form of high-crystalline-quality bulk crystals and thick epitaxial films.<sup>1–5</sup> This polymorph has a bandgap of  $\sim 4.85$  eV, with a breakdown field of 8 MV/cm, and electron saturation velocity of  $2 \times 10^7$  cm/s. For device applications, controllable n-type doping can be achieved with Sn or Si donors. It is not yet clear if extrinsic p-type doping can be achieved due to the formation of self-trapped holes. Large area bulk substrates are commercially available, and various types of devices, including Schottky diode power rectifiers, field effect transistors with Schottky or insulated gates, and high-sensitivity solar-blind photodetectors have been demonstrated. Since many of the expected applications of Ga<sub>2</sub>O<sub>3</sub> involve space-borne deployment, there is interest in its ability to withstand high radiation fluences of the type encountered in satellite or space applications and how it compares with materials like GaN.<sup>18–26</sup> These wide bandgap semiconductors have high bond strengths and hence vacancy formation energies. This means that they will have fewer atomic displacements per incoming nonionizing radiation particle than lower gap semiconductors.<sup>27–34</sup> The radiation hardness also depends on the type of defects created and their electrical activity.<sup>19</sup> For example, in n-type layers, the creation of compensating acceptors like Ga vacancies has a strong influence on the remaining net carrier concentration.<sup>19</sup> There are

already significant concentrations ( $>10^{18}$  cm<sup>-3</sup>) of ionized Ga vacancies in currently available Ga<sub>2</sub>O<sub>3</sub>, as determined by positron annihilation spectroscopy and electron paramagnetic resonance.<sup>35,36</sup>

There have been some recent reports on the effect of proton, electron, gamma ray, and neutron irradiation on devices and material properties of n-type  $\beta$ -Ga<sub>2</sub>O<sub>3</sub> under conditions relevant to space exposure conditions.<sup>22–27,37–39</sup> In general, the carrier concentration decreases due to trap formation as a result of radiation damage, the electron mobility degrades and this leads to changes in the performance of the rectifiers and UV photodetectors tested. The few reports of carrier removal rates in Ga<sub>2</sub>O<sub>3</sub> as a result of radiation exposure show them to be roughly comparable to those in GaN of similar doping levels for the same types of fluences.<sup>22–27</sup>

In this paper, we report the effect of 18 MeV alpha particle irradiation on vertical geometry  $\beta$ -Ga<sub>2</sub>O<sub>3</sub> Schottky rectifiers. The carrier removal rate is found to be  $\sim 406$ – $728$  cm<sup>-1</sup> for this energy, the highest reported for any of the radiation types examined to date.

## II. EXPERIMENT

The starting samples were bulk  $\beta$ -phase Ga<sub>2</sub>O<sub>3</sub> single crystal wafers ( $\sim 650$   $\mu$ m thick) with (001) surface orientation grown by the edge-defined film-fed growth method.<sup>1</sup> Hall measurements showed these Sn-doped wafers had carrier concentration of  $2.2 \times 10^{18}$  cm<sup>-3</sup>. Epitaxial layers (initially  $\sim 20$   $\mu$ m thick) of lightly Si-doped n-type Ga<sub>2</sub>O<sub>3</sub> ( $\sim 8.3 \times 10^{15}$  cm<sup>-3</sup>) were grown on these substrates by hydride vapor phase epitaxy. After growth, the episurface

<sup>a)</sup>Electronic mail: speart@mse.ufl.edu

was subjected to chemical mechanical polishing to planarize the surface, with a final epitaxial layer thickness of  $\sim 7 \mu\text{m}$ .

Vertical geometry, homoepitaxial diodes were fabricated by depositing a full area back Ohmic contacts of Ti/Au (20 nm/80 nm) by e-beam evaporation. The front sides were patterned by lift-off of electron-beam deposited circular Schottky contacts Ni/Au (20 nm/80 nm) with the diameter of  $210 \mu\text{m}$ . Figure 1 shows a schematic of the rectifier layer structure. Current–voltage (I–V) characteristics were recorded at  $25^\circ\text{C}$  on an Agilent 4145B parameter analyzer. The 18-MeV proton beam was generated using a MC-50 Cyclotron at the Korea Atomic Energy Research Institute. The alpha particle beam was injected into a low-vacuum chamber, where the  $\beta\text{-Ga}_2\text{O}_3$ -based devices were loaded, facing the beam. The average beam-current, measured by Faraday-cup, was 100 nA during the proton irradiation process. Fluences were fixed at  $10^{12}$  and  $10^{13} \text{ cm}^{-2}$ . The projected range of the 18-MeV alpha particle beam was calculated using the stopping and range of ions in matter (SRIM) program and is  $80 \mu\text{m}$ , as shown in Fig. 2. This means that the alpha particles completely traverse the drift region of the rectifiers and come to rest in the substrate. In other words, the damage is mainly beyond the drift region.

### III. RESULTS AND DISCUSSION

The forward and reverse bias I–V characteristics shown in Fig. 3 demonstrate that the alpha irradiation-induced damage is already measurable for the lowest dose. We can summarize the effects on the I–V characteristics as follows:

- (1) The barrier height and ideality factors showed little change at either dose, but the on-state resistance,  $R_{\text{ON}}$ , increased from 4 to  $62 \text{ m}\Omega\text{cm}^{-2}$  at the higher dose. The reverse breakdown voltage increased from 60 V in the reference to 80 and 110 V, respectively, in the  $10^{12}$  and  $10^{13} \text{ cm}^{-2}$  dose samples.
- (2) The carrier concentration in the drift region decreased as a result of alpha particle damage and led to an increase in reverse breakdown voltage. The decrease in net electron density in the epilayer results from the deep trap formation by nonionizing energy loss that compensates the initial donor doping. Previous experiments on proton irradiated  $\beta\text{-Ga}_2\text{O}_3$  nanobelts have shown that the electron mobility also decreases as a result of radiation damage.<sup>26</sup>

Quantification of the carrier loss can be obtained from  $1/C^2$ -V plots for the rectifiers after alpha particle irradiation shown in Fig. 4. The calculated carrier removal rate was  $406 \text{ cm}^{-1}$  for the  $10^{12} \text{ cm}^{-2}$  dose and  $728 \text{ cm}^{-1}$  for the

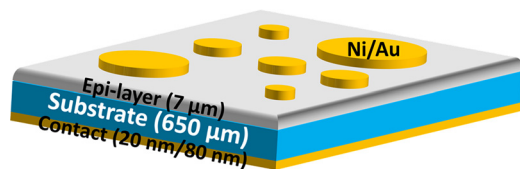


FIG. 1. (Color online) Schematic of vertical Ni/Au Schottky diode on  $7 \mu\text{m}$  thick  $\text{Ga}_2\text{O}_3$  epilayer doped at  $8.3 \times 10^{15} \text{ cm}^{-3}$  on a conducting  $\beta\text{-Ga}_2\text{O}_3$  substrate doped at  $2.2 \times 10^{18} \text{ cm}^{-3}$ .

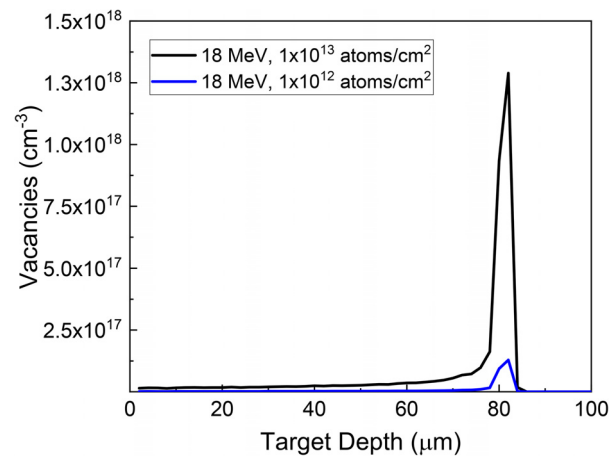


FIG. 2. (Color online) SRIM simulation of vacancy distribution in  $\text{Ga}_2\text{O}_3$  exposed to 18 MeV alpha particles to doses of  $10^{12}$  and  $10^{13} \text{ cm}^{-2}$ , respectively.

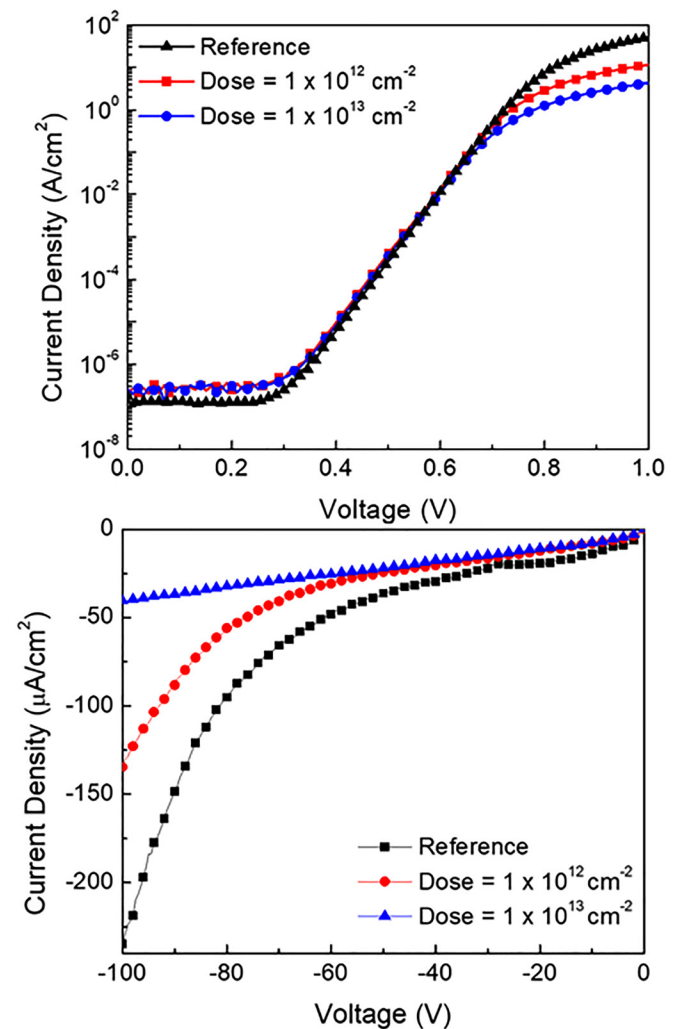


FIG. 3. (Color online) Forward (top) and reverse (bottom) current density–voltage characteristics before and after 18 MeV alpha particle irradiation with fluences of  $10^{12}$  or  $10^{13} \text{ cm}^{-2}$ .

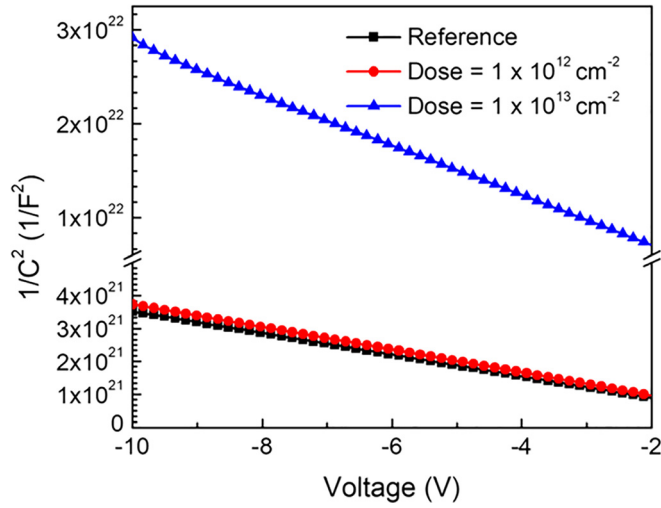


FIG. 4. (Color online)  $C^{-2}$ -V characteristics of  $\text{Ga}_2\text{O}_3$  rectifiers before and after alpha particle irradiation at two different doses.

$10^{13} \text{ cm}^{-2}$  dose. The initial carrier density of  $8.3 \times 10^{15} \text{ cm}^{-3}$  was reduced to  $7.9 \times 10^{15} \text{ cm}^{-3}$  after a dose of  $10^{12} \text{ cm}^{-2}$  and to  $1.03 \times 10^{15} \text{ cm}^{-3}$  after the higher dose of  $10^{13} \text{ cm}^{-2}$ .

Figure 5 shows the rectifier on/off ratio when switching from +1 V forward bias to the reverse voltages shown on the x-axis. The unirradiated rectifiers showed on/off ratios of  $>10^6$  across the entire voltage range investigated. These values were degraded by alpha particle irradiation, as summarized in Table I. This is due to the reduction of forward current as the carrier density is reduced by the alpha particle damage-induced trap introduction. These results show that some parameters of the rectifiers are more degraded by exposure to high energy alpha particle fluences than others, due to the specific loss of carriers and electron mobility.

Figure 6 shows a compilation of reported carrier removal rates for  $\text{Ga}_2\text{O}_3$ . The carrier removal rates for alpha particle irradiation of  $406\text{--}728 \text{ cm}^{-1}$  are the much higher than for

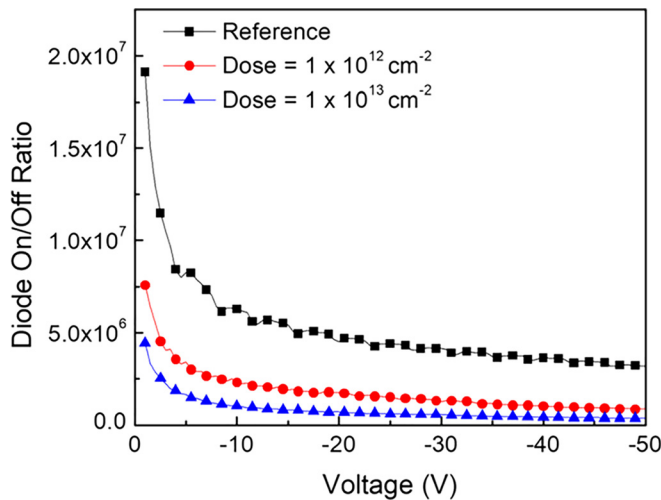


FIG. 5. (Color online) On/off ratio as a function of reverse bias voltage for rectifiers before and after proton irradiation and subsequent annealing at either 300 or 450 °C.

TABLE I. Summary of diode and drift region parameters before and after alpha particle irradiation.

Parameter	Reference	Dose ( $10^{12} \text{ cm}^{-2}$ )	Dose ( $10^{13} \text{ cm}^{-2}$ )
Barrier height (eV)	1.09	1.05	1.04
Ideality factor	1.03	1.09	1.10
$R_{\text{ON}}$ ( $\text{m}\Omega \text{ cm}^{-2}$ )	4.0	22	62
Drift region carrier concentration ( $\text{cm}^{-3}$ )	$8.3 \times 10^{15}$	$7.9 \times 10^{15}$	$1.03 \times 10^{15}$
Carrier removal rate ( $\text{cm}^{-1}$ )	n/a	406	728
Reverse recovery time (ns)	22	21	16
Reverse breakdown voltage (V)	60	80	110
On-off ratio ( $-1 \text{ V}$ )	$1.9 \times 10^7$	$7.5 \times 10^6$	$4.8 \times 10^6$

protons, neutrons, or electrons, reported previously. For example, carrier removal rates of  $\sim 4.9 \text{ cm}^{-1}$  for 1.5 MeV electron irradiation and  $\sim 300 \text{ cm}^{-1}$  for 10 MeV protons were reported for the same type of rectifiers.<sup>25</sup> Note that alpha particles exhibit the highest carrier removal rates of the four types of radiation represented. The results for  $\text{Ga}_2\text{O}_3$  are also generally comparable to those for GaN (Refs. 20 and 21) and indicate that the former is a good candidate for space-borne applications.

Finally, we also measured the reverse recovery characteristics when switching from +1 V to a range of reverse biases and found recovery times of order 20 ns for both control and alpha particle irradiated rectifiers, as shown in Fig. 7. The oscillations are due to the decay of stored charge upon switching bias polarities. This is consistent with both electron and proton irradiated rectifiers in which the reverse recovery showed little change with radiation dose,<sup>25</sup> since the minority carrier lifetime (which controls the carrier storage time in the intrinsic layer) is already small in  $\text{Ga}_2\text{O}_3$ .

Table I and the data shown in this paper emphasize that the diode parameters most affected by alpha particle irradiation are the on-state resistance, reverse breakdown voltage, and on-off ratio, while the diode ideality factor, barrier height, and reverse recovery do not show significant changes

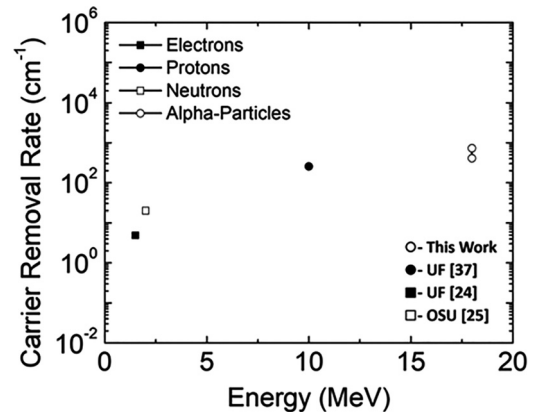


FIG. 6. Carrier removal rate for radiation damage of  $\text{Ga}_2\text{O}_3$  measured in this work and also reported previously, as a function of radiation type and energy. Similar data for various types of GaN-based high electron mobility transistors and thin films are shown for comparison.



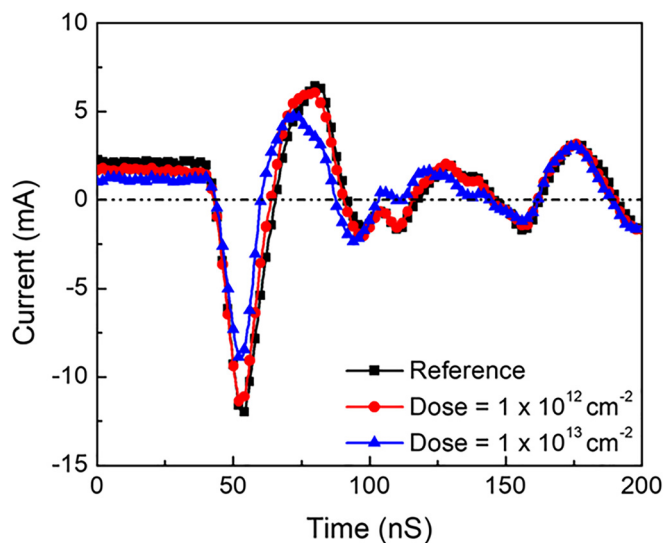


FIG. 7. (Color online) Reverse recovery characteristics of rectifiers before and after proton irradiation.

for the doses we investigated. Rectifiers are a convenient platform for investigating radiation effects since they have a simple structure but yield a large number of measurable device parameters.

#### IV. SUMMARY AND CONCLUSIONS

Ga<sub>2</sub>O<sub>3</sub> rectifiers were irradiated with 18 MeV alpha particles at fluences of  $10^{12}$ – $10^{13}$  cm<sup>-2</sup>. The carrier removal rate in the drift region of the rectifiers was 406–728 cm<sup>-1</sup> under these conditions. The reverse breakdown voltage increases in response to a reduction in channel carrier density, and the on/off ratio is also degraded. The carrier removal rates in Ga<sub>2</sub>O<sub>3</sub> are comparable to those in GaN under similar conditions.

#### ACKNOWLEDGMENTS

This project was sponsored by the Department of the Defense, Defense Threat Reduction Agency, HDTRA1-17-1-011, monitored by Jacob Calkins. The content of the information does not necessarily reflect the position or the policy of the federal government, and no official endorsement should be inferred. The research at Korea University was supported by the New and Renewable Energy Core Technology Program of the Korea Institute of Energy Technology Evaluation and Planning (KETEP) grant from the Ministry of Trade, Industry and Energy, Republic of Korea (20173010012970 and 20172010104830). Part of the work at Tamura was supported by “The research and development project for innovation technique of energy conservation” of the New Energy and Industrial Technology Development Organization (NEDO), Japan. The authors also thank Kohei Sasaki from Tamura Corporation for fruitful discussions.

<sup>1</sup>A. Kuramata, K. Koshi, S. Watanabe, Y. Yamaoka, T. Masui, and S. Yamakoshi, *Jpn. J. Appl. Phys., Part 1* **55**, 1202A2 (2016).

- <sup>2</sup>S. J. Pearton, J. Yang, P. H. Cary IV, F. Ren, J. Kim, M. J. Tadjer, and M. A. Mastro, *App. Phys. Rev.* **5**, 011301 (2018).
- <sup>3</sup>S. I. Stepanov, V. I. Nikolaev, V. E. Bougrov, and A. E. Romanov, *Rev. Adv. Mater. Sci.* **44**, 63 (2016), see [http://www.ipme.ru/e-journals/RAMS/no\\_14416/06\\_14416\\_stepanov.pdf](http://www.ipme.ru/e-journals/RAMS/no_14416/06_14416_stepanov.pdf).
- <sup>4</sup>M. A. Mastro, A. Kuramata, J. Calkins, J. Kim, F. Ren, and S. J. Pearton, *ECS J. Solid State Sci. Technol.* **6**, P356 (2017).
- <sup>5</sup>H. Von Wenckstern, *Adv. Electron. Mater.* **3**, 1600350 (2017).
- <sup>6</sup>J. Y. Tsao *et al.*, *Adv. Electron. Mater.* **4**, 1600501 (2018).
- <sup>7</sup>M. Higashiwaki and G. H. Jessen, *Appl. Phys. Lett.* **112**, 060401 (2018).
- <sup>8</sup>M. J. Tadjer *et al.*, *Phys. Status Solidi A* **213**, 893 (2016).
- <sup>9</sup>M. Kim, J.-H. Seo, U. Singiseti, and Z. Ma, *J. Mater. Chem. C* **5**, 8338 (2017).
- <sup>10</sup>S. Rafique, L. Han, and H. Zhao, *ECS Trans.* **80**, 203 (2017).
- <sup>11</sup>M. J. Tadjer *et al.*, *J. Electron. Mater.* **45**, 2031 (2016).
- <sup>12</sup>S. Rafique, L. Han, M. J. Tadjer, J. A. Freitas, Jr., N. A. Mahadik, and H. Zhao, *Appl. Phys. Lett.* **108**, 182105 (2016).
- <sup>13</sup>M. Higashiwaki, K. Sasaki, H. Murakami, Y. Kumagai, A. Koukitu, A. Kuramata, T. Masui, and S. Yamakoshi, *Semicond. Sci. Technol.* **31**, 034001 (2016).
- <sup>14</sup>A. J. Green *et al.*, *IEEE Electron Device Lett.* **37**, 902 (2016).
- <sup>15</sup>M. H. Wong, K. Sasaki, A. Kuramata, S. Yamakoshi, and M. Higashiwaki, *IEEE Electron Device Lett.* **37**, 212 (2016).
- <sup>16</sup>M. J. Tadjer, N. A. Mahadik, V. D. Wheeler, E. R. Glaser, L. Ruppalt, A. D. Koehler, K. D. Hobart, C. R. Eddy, Jr., and F. J. Kub, *ECS J. Solid State Sci. Technol.* **5**, 468 (2016).
- <sup>17</sup>K. D. Chabak *et al.*, *Appl. Phys. Lett.* **109**, 213501 (2016).
- <sup>18</sup>E. R. Benton and E. V. Benton, *Nucl. Instrum. Methods Phys. Res., B* **184**, 255 (2001).
- <sup>19</sup>B. D. Weaver, T. J. Anderson, A. D. Koehler, J. D. Greenlee, J. K. Hite, D. I. Shahin, F. J. Kub, and K. D. Hobart, *ECS J. Solid State Sci. Technol.* **5**, Q208 (2016).
- <sup>20</sup>S. J. Pearton, F. Ren, E. Patrick, M. E. Law, and A. Y. Polyakov, *ECS J. Solid State Sci. Technol.* **5**, Q35 (2016).
- <sup>21</sup>S. J. Pearton, R. Deist, F. Ren, L. Liu, A. Y. Polyakov, and J. Kim, *J. Vac. Sci. Technol., A* **31**, 050801 (2013).
- <sup>22</sup>S. Ahn *et al.*, *J. Vac. Sci. Technol., B* **34**, 041213 (2016).
- <sup>23</sup>D. Szalkai, Z. Galazka, K. Irscher, P. Tüttő, A. Klíx, and D. Gehre, *IEEE Trans. Nucl. Sci.* **64**, 1574 (2017).
- <sup>24</sup>J. Yang, F. Ren, S. J. Pearton, G. Yang, J. Kim, and A. Kuramata, *J. Vac. Sci. Technol., B* **35**, 031208 (2017).
- <sup>25</sup>A. A. Arehart, E. Farzana, T. E. Blue, and S. A. Ringel, paper presented at 2nd International Workshop on Ga<sub>2</sub>O<sub>3</sub> and Related Materials, Parma, Italy, September (2017).
- <sup>26</sup>G. Yang, S. Jang, F. Ren, S. J. Pearton, and J. Kim, *ACS Appl. Mater. Interfaces* **9**, 40471 (2017).
- <sup>27</sup>J. Yang *et al.*, *J. Vac. Sci. Technol., B* **35**, 051201 (2017).
- <sup>28</sup>K. Konishi, K. Goto, H. Murakami, Y. Kumagai, A. Kuramata, S. Yamakoshi, and M. Higashiwaki, *Appl. Phys. Lett.* **110**, 103506 (2017).
- <sup>29</sup>S. Ahn, F. Ren, L. Yuan, S. J. Pearton, and A. Kuramata, *ECS J. Solid State Sci. Technol.* **6**, P68 (2017).
- <sup>30</sup>T. J. Anderson, A. D. Koehler, J. D. Greenlee, B. D. Weaver, M. A. Mastro, J. K. Hite, C. R. Eddy, F. J. Kub, and K. D. Hobart, *IEEE Electron Device Lett.* **35**, 826 (2014).
- <sup>31</sup>J. D. Greenlee *et al.*, *Appl. Phys. Lett.* **107**, 083504 (2015).
- <sup>32</sup>T. J. Anderson, A. D. Koehler, J. A. Freitas, Jr., B. D. Weaver, J. D. Greenlee, M. J. Tadjer, E. A. Imhoff, K. D. Hobart, and F. J. Kub, *ECS J. Solid State Sci. Technol.* **5**, Q289 (2016).
- <sup>33</sup>T. J. Anderson, D. J. Meyer, A. D. Koehler, J. A. Roussos, B. D. Weaver, K. D. Hobart, and F. J. Kub, *ECS J. Solid State Sci. Technol.* **6**, S3110 (2017).
- <sup>34</sup>J. C. Gallagher, T. J. Anderson, A. D. Koehler, N. A. Mahadik, A. Nath, B. D. Weaver, K. D. Hobart, and F. J. Kub, *ECS J. Solid State Sci. Technol.* **6**, S3060 (2017).
- <sup>35</sup>E. Korhonen, F. Tuomisto, D. Gogova, G. Wagner, M. Baldini, Z. Galazka, R. Schewski, and M. Albrecht, *Appl. Phys. Lett.* **106**, 242103 (2015).
- <sup>36</sup>B. E. Kananen, L. E. Halliburton, K. T. Stevens, G. K. Foundos, K. B. Chang, and N. C. Giles, *Appl. Phys. Lett.* **110**, 202104 (2017).
- <sup>37</sup>J. Yang *et al.*, *J. Vac. Sci. Technol., B* **36**, 011206 (2018).
- <sup>38</sup>A. Y. Polyakov *et al.*, *Appl. Phys. Lett.* **112**, 032107 (2018).
- <sup>39</sup>J. D. Lee, E. Flitsyan, L. Chernyak, J. Yang, F. Ren, S. J. Pearton, B. Meyler, and Y. J. Salzman, *Appl. Phys. Lett.* **112**, 082104 (2018).